FULL PAPER

Proton Conducting Phase-Separated Multiblock Copolymers with Sulfonated Poly(phenylene sulfone) Blocks for Electrochemical Applications: Preparation, Morphology, Hydration Behavior, and Transport

*Giorgi Titvinidze, Klaus-Dieter Kreuer, Michael Schuster, Carla C. de Araujo, Jan P. Melchior, and Wolfgang H. Meyer**

A family of multiblock copolymers consisting of alternating fully sulfonated hydrophilic poly(phenylene sulfone) and hydrophobic poly(phenylene ether sulfone) segments are prepared and characterized. The multiblock copolymers are formed by the coupling of preformed hydrophilic and hydrophobic blocks using a specially designed coupling agent. The block lengths (degree of polymerization) of both segment types were varied in order to control the ion exchange capacity. Solution cast films show spontaneous nanophase separation leading to distinct bicontinuous morphologies with correlation lengths around 15 nm. The hydrophobic phase gives the membranes their advantageous viscoelastic properties even at high temperatures under both wet and dry conditions, while proton conductivity takes place within the hydrophilic phase. Since the properties of fully sulfonated poly (phenylene sulfone)s are locally preserved within the hydrophilic domain, the membranes show very high proton conductivity and high hydrolytic stability. The very high degree of water dispersion within the hydrophilic domains leads to very low electro-osmotic water drag. Because of their superior transport and stability properties these multiblock copolymers have a great potential for use as a substitute for perfluorosulfonic acid membranes which are used as separator materials in electrochemical applications such as polymer electrolyte membrane (PEM) fuel cells and redox flow batteries.

1. Introduction

Although perfluorosulfonic acid (PFSA) and even sulfonated hydrocarbon membranes are successfully used as separator materials in polymer electrolyte membrane fuel cells (PEMFC), the properties of such materials still limit the conditions under which PEM fuel cells can be operated. This has mainly to do with transport (proton conductivity and water transport) and stability issues. PFSA membranes suffer from a loss of mechanical strength with increasing temperature, high gas permeability leading to the formation of aggressive radicals at the catalyst surface,[1] a very high electro-osmotic drag of water,[2] and a severe decay of proton conductivity at high temperature and low levels of humidification.[3,4]

Since the membrane properties and the complexity and cost of fuel cell systems are closely related,[5] there is a clear need for optimized or conceptually new types of membrane.

Many approaches rely on the properties of aromatic hydrocarbon polymers, and, based on this, membranes with encouraging properties have been reported. However, the performance at high temperature and low relative humidity (RH) was always found to be the same or worse than for PFSA membranes,[6–10] which is mainly explained by microstructural differences between these two families of membrane material.[6,11] Some partially sulfonated random copolymers already show improved conductivities over PFSA membranes at high RH, but this is lost at low RH.[12]

At this stage, the most promising approach for overcoming the limited proton conductivity at low RH and high temperatures appears to be hydrophilic-hydrophobic multiblock copolymers.[13–24] Such multiblock copolymers with sulfonic acid functionalized hydrophilic blocks and unfunctionalized hydrophobic blocks display nano-phase (≈10–100 nm) separated bicontinuous morphologies. Proton transport in the hydrophilic domains is high, even at low RH and high temperatures. This is because the water structures within their sub-nano-sized water domains are still well connected under these conditions, which is a consequence of the high local density of sulfonic acid functional groups. The nonionic domains provide dimensional stability and mechanical strength.[25,26]

Dr. G. Titvinidze, Dr. W. H. Meyer
Max Planck Institute for Polymer Research
Ackermannweg 10, 55128 Mainz, Germany
E-mail: meyer@mpip-mainz.mpg.de
Dr. K. D. Kreuer, Dr. C. C. de Araujo, J. P. Melchior
Max Planck Institute for Solid State Research
Heisenbergstr. 1, 70569 Stuttgart, Germany
Dr. M. Schuster
FuMaTech GmbH
Am Grubenstollen 11, 66368 St. Ingbert, Germany

DOI: 10.1002/adfm.201200811

However, despite the successful development of numerous multiblock copolymers, their long term hydrolytic stability is questionable, since the sulfonic acid groups are usually introduced via post-sulfonation at the ortho position to electron donating ether linkages,[6,23,24]] which leads to lower stability.[27] In order to improve long-term stability Jannasch and co-workers designed multiblock copolymers with highly sulfonated blocks with $-SO_3H$ in ortho position to the strongly electron withdrawing sulfone bridge.[28,29] However, these polymers were obtained by post-sulfonation via lithiation, a reaction path which is more sensitive and in which undesired side reactions may occur and the degree of sulfonation is not easy to control. Thus, for commercial application direct copolymerization of sulfonated monomers seems us to be the more appropriate approach.[6,30–32]

Recently, we reported on the synthesis and properties of novel multiblock copolymers based on fully sulfonated (phenylene sulfone) blocks made from sulfonated monomers.[33] The present full paper gives all corresponding details.

Polysulfone blocks (SU_v), in which each phenyl ring is monosulfonated, were chosen as hydrophilic part, and arylethersulfone blocks (ES_w, FS_w) were chosen as the hydrophobic part to achieve phase separation on the basis of a high hydrophilic-hydrophobic contrast (**Table 1**).

The SU_v-blocks are advantageous over frequently reported sulfonated poly(arylene ether sulfone)s due to their higher stability against desulfonation. The stabilization effect is caused by the presence of electron-withdrawing groups (-SO_2-) in the ortho position to the sulfonic acid groups.[27,34,35] In earlier publications the preparation and properties of pure SU_v-polymers (in the following termed *"S-220"*, where 220 refers to the equivalent weight of 220 g eq^{-1} corresponding to an IEC of 4.5 meq g^{-1}) were reported in detail.[34,35] SU_v-blocks were synthesized by direct copolymerization of sulfonated monomers. As compared to the post-sulfonation route, the direct copolymerization allows for the exact control of the degree of sulfonation and decreases the possibility of side reactions that can occur during polymer analogous post-sulfonation processes.

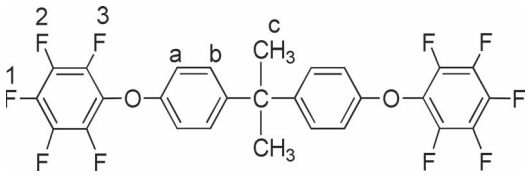

Scheme 1. Chemical structure of the coupling agent "BPAF10" used for end-functionalization of the hydrophilic blocks (SU_v) and coupling to the hydrophobic blocks (ES_w, FS_w).

The need for highly reactive end-groups for coupling the hydrophilic with the hydrophobic blocks is reported in the literature.[15,24] Such end-groups allow for the coupling of the preformed blocks at moderate temperatures, which in turn prevent ether-ether interchange reactions[36] and lead to high molecular weights of the multiblock copolymers.[37] Typically, the reactive end-groups are attached to the hydrophobic blocks, while the synthetic route described here uses the end-group functionalization of the hydrophilic blocks with a newly designed coupling agent [bisphenol-A-bis (penta-fluoro-phenyl)ether, BPAF10]. This allows a lower coupling temperature and the determination of the hydrophilic block length via ^{1}H-NMR on the basis of its methyl group signals (c) (**Scheme 1**).

While the IEC of the hydrophilic blocks (SU_v) is fixed in this work (IEC = 4.5 meq g^{-1}) the IEC of the present multiblock copolymers is lower depending on the ratio of the mass

Table 1. Chemical structure of the repeat units of the hydrophilic and hydrophobic blocks and their names used in this publication.

Chemical Structure of Block Repeat Units	Block name	M[a)]	Remarks
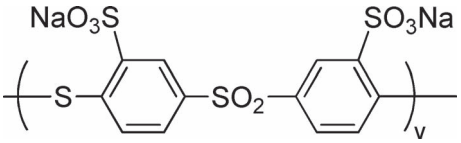	SS_v	452	Hydrophilic sulfonated aryl sulfone-sulfide precursor
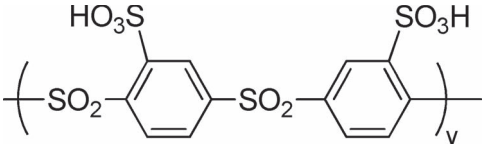	SU_v	440	Hydrophilic sulfonated aryl sulfone (acid form)
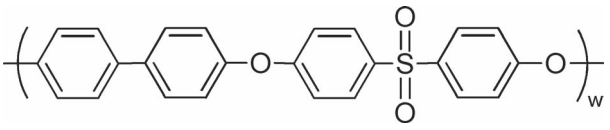	ES_w	400	Hydrophobic aryl ether sulfone
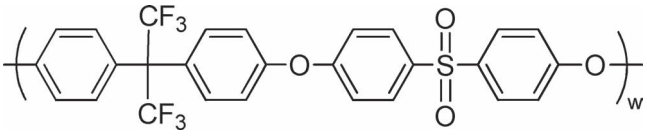	FS_w	550	Hydrophobic aryl ether sulfone

[a)]Molecular weight of repeat unit; v, w: average number of repeat units in the block.

increments of the hydrophilic and hydrophobic blocks. This is expressed as v/w (with v, w the average number of repeat units in the hydrophilic and hydrophobic blocks, respectively).

Apart from this ratio, the absolute numbers of v and w (block lengths) and the number of hydrophilic-hydrophobic block sequences (z) are expected to influence the ability to phase-separate into nano-sized domains. Therefore, the values for v, w and z of structures such as $[SU_v\text{-}ES_w]_z$ and $[SU_v\text{-}FS_w]_z$ are given in the present work.

This paper presents a series of multiblock copolymers with IEC = 1.2–1.7 meq g^{-1}, their preparation and characterization with respect to morphological, thermodynamical and transport properties. The data are compared to those of the PFSA ionomer Nafion measured under the same experimental conditions.

2. Experimental Section

2.1. Materials

Disodium-3,3′-disulfonate-4,4′-difluorodiphenylsulfone was purchased from Fumatech GmbH (Germany). Before use it was dried at T = 150 °C in vacuum. Anhydrous potassium carbonate (99%, Acros Organics), bis-(4-chlorophenyl)-sulfone (98%, Aldrich), 2,2′-bis (4-hydroxyphenyl)hexafluoropropane (BHFP) (98%, Aldrich), hexafluorobenzene (HFB) (99%, Acros Organics), 4,4′-dihydroxybiphenyl (BP) (99%, Aldrich), Bisphenol A (99%, Aldrich), lithium sulfide (99.9%, Alfa Aesar), *N*-methyl-2-pyrrolidone (NMP) (99.5%, extra dry stored over molecular sieve, water < 50 ppm, Acros Organics), dimethyl sulfoxide (DMSO) (99.9%, Aldrich), *N*,*N*-dimethylacetamide (DMAc) (anhydrous, 99.8%, Aldrich) and toluene (99.8%, Aldrich) were used without further purification.

2.2. Measurements

2.2.1. NMR Analysis

^1H, ^{13}C and ^{19}F NMR spectra were recorded using Bruker Avance 250 MHz, Bruker Avance DRX 300 MHz and Bruker DSX500 spectrometers at room temperature with deuterated dimethyl sulfoxide (DMSO-d_6) as a solvent. For ^1H and ^{13}C NMR spectra DMSO-d_6 was used as an internal standard, while for ^{19}F NMR spectra HFB was taken as a standard.

2.2.2. Molecular Weights

Molecular weights were determined by gel permeation chromatography (GPC) using a Waters 515 system equipped with three consecutive columns (GRAM, 10 000, 1 000, 100, Polymer Standard Service) calibrated with polystyrene (Polymer Standard Service, Germany), equipped with a UV detector (Soma S-3702) and RI detector (ERC 7512; ERMA). The GPC measurements were performed in DMF at 60 °C with an addition of LiBr (1 g l^{-1}).

2.2.3. Thermoanalysis

Thermogravimetric Analysis (TGA) was carried out on a TGA/SDTA-851 (Mettler-Toledo, Germany) in nitrogen gas at a heating rate of 10 K min^{-1}. Before analysis, the films were dried in a vacuum at 120 °C for at least 48 h to remove absorbed water. Differential scanning calorimetry (DSC) was carried out on a Mettler-Toledo DSC-30 in nitrogen gas at a heating rate of 10 K min^{-1}. DSC analyses were performed with both, the Na-form as well the H-form of the multiblock copolymers, but a Tg was never observed.

2.2.4. Dynamical Mechanical Analysis (DMA)

DMA was performed on a DMA Q 800 (TA Instruments) connected to a homebuilt humidifier with temperature and relative humidity (RH) as parameters. The sample holder was hermetically encapsulated,[38] and RH was controlled by keeping the temperature of the humidifier and the sample constant within ±0.05 °C. Nitrogen was used as a transport gas at a flow rate of 40 mL/min, and the capillary connecting humidifier and sample holder were kept at a temperature 20 °C above the sample temperature. For each set of conditions temperature and RH were kept constant for a minimum of five hours while continuously recording data. The measurements were performed by applying oscillatory sinusoidal tensile deformation with a frequency of ν = 1 Hz, an amplitude of A = 5 μm and a preload force of F = 0.01 N on a rectangular film sample of 20 × 5 × 0.05–0.2 mm.

2.2.5. Hydration Behavior, Swelling

Water hydration isobars were determined by thermogravimetric analysis (TGA) using a homebuilt humidifier. A Mettler AT 20 balance was magnetically coupled (Rubotherm) to a crucible. This allowed us to record weight changes under high RH conditions while avoiding condensation of water in the instrument. Temperatures of the humidifier and the sample were controlled with an accuracy of ±0.05 K, and the carrier gas nitrogen was used at a flow rate of 40 ml/min. Depending on the T/RH conditions, samples were allowed to equilibrate between 5 and 20 h while data points were continuously recorded. The measurements started at a high relative humidity (RH = 95%) with subsequent heating and cooling runs. Since the data were found to be quasi reversible (for RH < 80%) and reproducible, hydration isotherms could reliably be extracted from these data.

For measuring the degree of hydration in pure water atmosphere (p_{H2O} = 1 atm) in the range 103 ≤ T ≤ 160 °C, water was injected into the system via an evaporation system at the rate of 20 μL/min using a peristaltic pump.

The swelling in water was determined by measuring the weight gain of immersed membrane pieces treated in an autoclave half filled with water for two hours. The weights of the dry samples were taken as a reference. The results were significantly less reproducible than the hydration behavior at a constant RH and particularly depended on the pre-treatment of the membrane pieces. Here, we only show the swelling after standardization at T = 80 °C in 1 M sulfuric acid and pure water.

2.2.6. AFM and TEM Characterization

Tapping mode AFM observations were performed by a Dimension 3100 Atomic Force Microscope, using Olympus tapping mode cantilevers OMCL-AC 160 TS-W2 with a force constant of

42 N/m and resonance frequency of around 300 kHz. All images were taken under ambient conditions (RH ≈ 50%) (Veeco, USA).

The membrane morphology was also characterized by transmission electron microscopy (TEM). For TEM examination the sample films were sectioned at room temperature with a Leica Ultracut UCT ultramicrotome equipped with a Diatome 35° diamond knife to a nominal thickness of approximately 60 nm. The sections were transferred to a Cu TEM grid and inspected with a FEI Tecnai F20 transmission electron microscope without further treatment at an acceleration voltage of 200 kV.

2.2.7. Small Angle X-Ray Scattering

Samples for SAXS experiments (four membrane slices of 40–60 µm thickness) were equilibrated at a fixed RH of 75% and then transferred into a gas tight brass cell with two thin Mylar sheets serving as windows. SAXS experiments were performed at the DUBBLE beam line (BM 26B) at the European Synchrotron Radiation Facility (ESRF) in Grenoble (France). The data were collected using a 2D multiwire gas-filled detector with pixel array dimensions of 512 × 512. The *q*-scale was calibrated using the position of diffracted peaks from a standard silver behenate powder. The exposure time for each sample was about 60 s and a wavelength of λ = 1.54 Å was applied. The experimental data were corrected for background scattering and transformed into 1D-plots by azimuthal angle integration.

2.2.8. Conductivity Measurements

Proton conductivities were obtained by ac-impedance spectroscopy (HP-ac-impedance analyzer 4192A LF) using a two-electrode set-up. The measurements were performed in a closed cell with pre-equilibrated samples (pressed stacks of 10–30 slices of each membrane with pre-adjusted water content, diameter ≈4 mm, thickness 2–5 mm) with gold electrodes. Accordingly, we measured conductivity as a function of temperature but for a constant degree of hydration (λ = const.).

In-plane conductivities were measured in pure water vapor ($p_{H2O} = 10^5$ Pa) with a four electrode set-up using a modified commercial conductivity cell (Fumatech).

2.2.9. Water Diffusion Coefficient and Electro-Osmotic Drag

PFG-NMR diffusion studies were carried out using a wide bore Oxford magnet operating at a magnetic field of 4.7 T and a Bruker Biospin NMR spectrometer operating at 200.1 MHz for ^{1}H. Magnetic field gradients were generated using a diff60 diffusion probe and a Great60 gradient amplifier (Bruker Biospin). Diffusion measurements were performed using the standard PFG NMR stimulated echo pulse sequence. The diffusion time was typically 10 ms and the gradient pulse width 1 ms.

The same spectrometer was used to measure electro-osmotic drag coefficients. During the NMR spin echo pulse sequence a proton current was drawn through the sample located in the NMR radio frequency coil, which caused an electro-osmotic flow of water in the same direction. This transport of water protons in the direction of the magnetic field gradient leads to a change in the Larmor precession frequency of their proton spins, which is detected as a phase shift. From this phase shift as a function of protonic current the electroosmotic water drag K_{drag} was calculated following the procedure of Ise et al.[39] The magnitude of the pulsed field gradient was varied between 70 and 130 G cm^{-1}; the diffusion time Δ between two pulses was varied between 18 and 22 ms, and the pulse duration δ was varied between to 1 and 1.3 ms. The recycling time in the E-NMR experiments was set to 140 s and the maximum current to 400 mA in order to avoid significant heat accumulation.

A typical complete experiment contained around 10 steps (0.1–0.3 A), repeated four times. The maximum voltage driving the current through the sample was approximately 20–60 V depending on the sample resistance which increases with decreasing water content. The polarity of the current was alternated between consecutive scans to avoid a water concentration gradient build up (drying out of one of the sample sides).

2.3. Synthesis

2.3.1. Bisphenol-A-bis (pentafluorophenyl) Ether (BPAF10)

Bisphenol-A (10 000 g, 43.8 mmol), HFB (32.590 g, 175.2 mmol), potassium carbonate (18.141 g, 131.4 mmol) and NMP (25 ml) were charged in a stainless steel autoclave (250 mL) equipped with a magnetic stirrer. After treatment of this mixture at 120 °C for 16 h the product was collected and purified by column chromatography (SiO_2, petrol ether: dichloromethane = 5:1 v/v) yielding 16.0 g (65%) white powder. (NMR data and other analytical details: see DATA at the end of paper).

2.3.2. Sulfonated Poly(phenylene sulfide sulfone) Precursor Block (SSv) End-Functionalized with BPAF10

Disodium 3,3′-disulfonate- 4,4′-difluorodiphenylsulfone (5.000 g, 10.92 mmol), lithium sulfide (0.550 g, 12.01 mmol) and anhydrous NMP (37 mL) were charged into a round-bottom flask in an Ar atmosphere. The reaction mixture was heated and stirred at 190 °C for 4 h, and then cooled to RT. *BPAF10* (2.5 g dissolved in 5 mL NMP) was added to end-functionalize the hydrophilic block. The temperature was slowly raised to 80 °C and kept overnight. After cooling to RT, the reaction mixture was precipitated in i-propanol and filtered. In order to remove all by- and low-molecular products, the mixture was dissolved in water and dialyzed against pure water for 24 h (dialysis tubing cellulose ester membrane, 1000 MWCO, Spectra/Por Biotech). After removal of the solvent by freeze-drying the yield was 4.421 g (89.5%). By varying the monomer ratio hydrophilic precursor blocks SS_v with different molecular weights were obtained. (NMR data: see Section 5. Experimental Data, **Scheme 2** and **Figure 1**a,c).

2.3.3. Sulfonated Poly(phenylene sulfone) Block (SUv) End-Functionalized with BPAF10

SS_v (end-functionalized with BPAF10, Na-form) (4.000 g) was suspended in glacial acetic acid (40 mL) at 70 °C. Hydrogen peroxide (10 mL 35% H_2O_2 in water) was slowly added to the reaction mixture. The reaction was kept at 70 °C for 10 h and additionally for 24 h at RT.

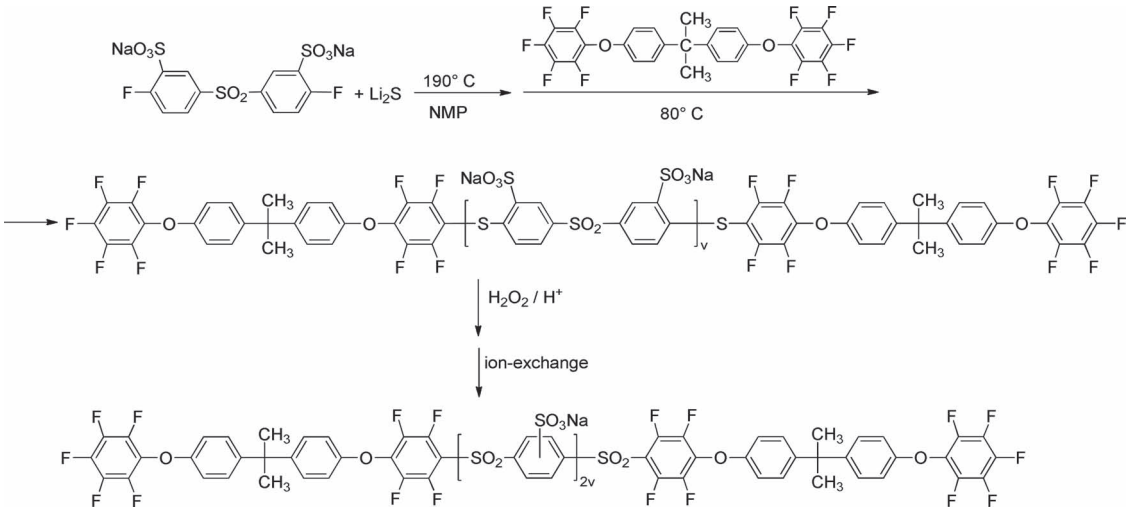

Scheme 2. Synthesis scheme of the hydrophilic blocks SS_v and SU_v.

Then the acetic acid was distilled off in a vacuum and the product was dialyzed for 24 h against pure water (Scheme 2 and **Table 2**). After dialysis, the sodium form was obtained by ion-exchange using an ion-exchange resin amberlite IR120 (plus). The water was finally removed by freeze-drying, yielding a white polymer (4.031 g, 95%). (NMR data: see Section 5. Experimental Data and Figure 1b,d).

2.3.4. Poly(arylene ether sulfone) Block (ES_w)

ES_w was synthesized according to the procedure described in the literature (**Scheme 3**)[10]: DCDPS (4.000 g, 13.93 mmol), BP (2.810 g, 15.08 mmol) and K_2CO_3 (2.501 g, 18.10 mmol) were charged into a round-bottom flask equipped with a Dean Stark trap, condenser, stirrer and gas adapter. DMAc (36 mL) and toluene (18 mL) were added in an Ar atmosphere. The reaction mixture was dehydrated at 150 °C for 4 h with refluxing toluene. After removing the toluene, the reaction temperature was slowly increased to 170 °C and kept constant for 48 h. After cooling to RT the product was precipitated in methanol and washed several times with water. The product was dried in vacuum at 120 °C for 48 h (Table 2). (NMR data: see Section 5. Experimental Data at the end of the paper).

2.3.5. Poly(arylene ether sulfone) Block (FS_w)

The synthesis of FS_w follows a procedure adapted from the literature (Scheme 3)[17]: DCDPS (4.000 g, 13.93 mmol), BHFP (5.070 g, 15.09 mmol) and K_2CO_3 (3.130 g, 22.64 mmol) were charged into a round-bottom flask equipped with a Dean Stark trap, condenser, stirrer and gas adapter. NMP (45 mL) and toluene (28 mL) were added in an Ar atmosphere. The reaction mixture was dehydrated at 150 °C for 4 h with refluxing toluene. After removal of the toluene, the reaction temperature was slowly increased to 180 °C and kept constant for 14 h. After cooling to RT the product was precipitated in methanol and washed several times with water. The product was dried in a vacuum at 120 °C for 48 h. By varying the monomer ratios, FS_w blocks with different molecular weights were obtained (Table 2). (NMR data: see Section 5. Experimental Data).

2.3.6. Multiblock Copolymers $[SU_v\text{-}ES_w]_z$ and $[SU_v\text{-}FS_w]_z$

The multiblock copolymers were synthesized by a multiple sequential coupling between the BPAF10 end-functionalized hydrophilic and phenoxide terminated hydrophobic blocks (**Scheme 4**). The stoichiometric ratio of the reactants was set on the basis of the molecular weights of the hydrophilic and hydrophobic blocks obtained from ^1H NMR. A typical procedure for the coupling reaction is as follows: SU_{14} (1.800 g, 0.244 mmol), FS_{15} (2.020 g, 0.244 mmol) and K_2CO_3 (0.140 g, 0.976 mmol) were charged into a round-bottom flask equipped with condenser, stirrer and gas adapter. DMSO (25 ml) were added to the flask in an Ar atmosphere. The mixture was heated to 70 °C and kept constant for 18 h. After the reaction was completed the solution was poured into i-propanol to precipitate the multiblock copolymer. The polymer was washed with water and subsequently with acetone. The reaction yield was typically 92%. By combining the different hydrophilic and hydrophobic blocks a small family of multiblock copolymers with different IECs was obtained (**Table 3**).

2.4. Membrane Preparation

The sodium-form multiblock copolymers were dissolved in DMSO (10 wt%), filtered with syringe filters (5 µm Teflon), cast onto dust free glass plates (Petri dishes) and dried at 70 °C in vacuum for 48 h. The acid-form was obtained by boiling the membranes in a 10 wt% aqueous solution of sulfuric acid for 8 h. Afterwards, the membranes were washed several times with deionized water, boiled in it for 8 h and stored in it at RT for further characterization.

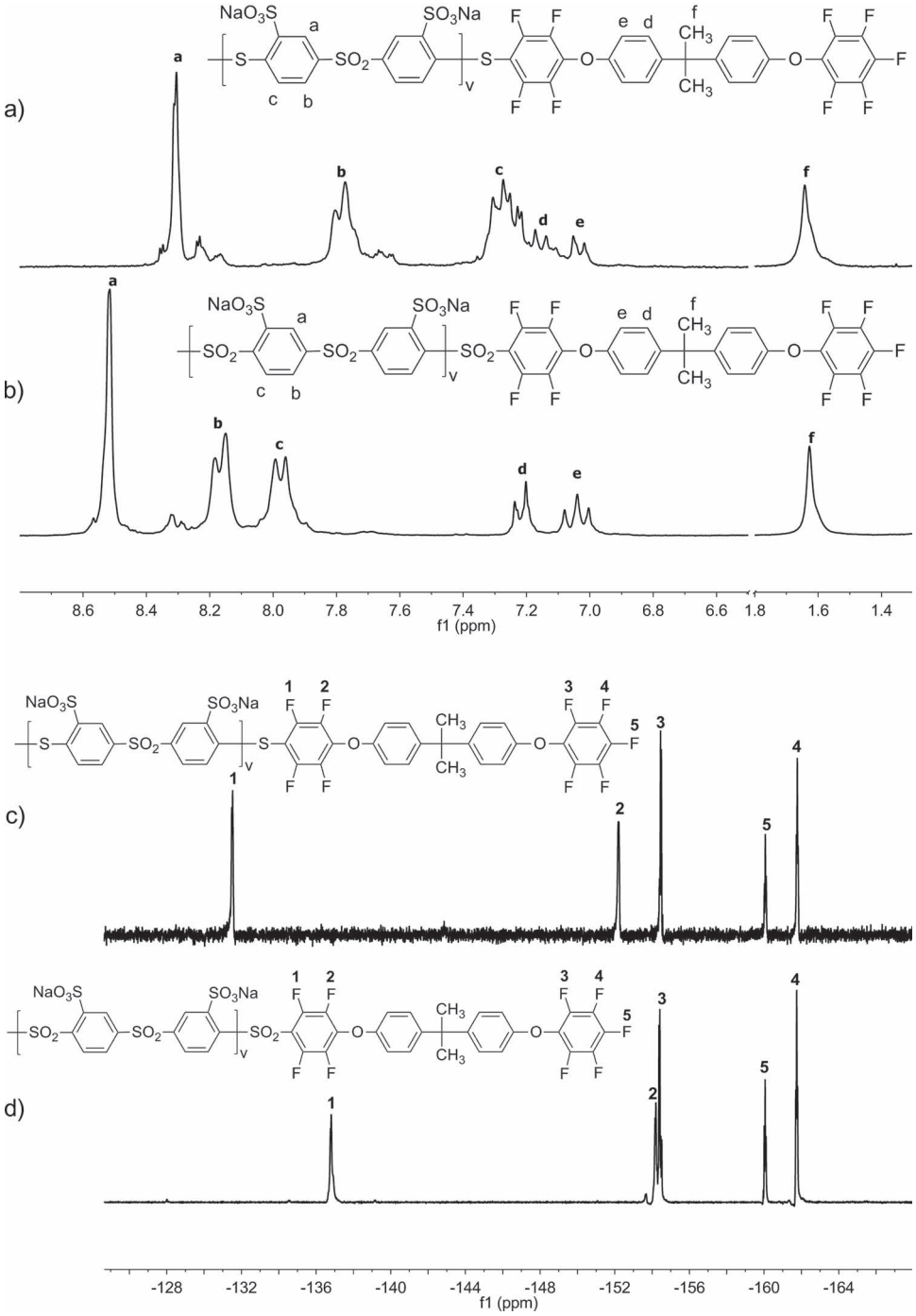

Figure 1. ^{1}H-NMR of the precursor block SS_v (a) and the hydrophilic block SU_v (b). Corresponding ^{19}F-NMR spectra (c,d).

3. Results and Discussion

3.1. Hydrophilic Blocks

The synthesis of the hydrophilic blocks was carried out in a three-step process comprising: 1) step growth polymerization to yield the precursor blocks SS_v 2) end-functionalizing SS_v with BPAF10 and 3) oxidation of SS_v to SU_v (Scheme 2).

In the first synthetic step a nucleophilic substitution reaction of disodium 3,3′-disulfonate-4,4′-difluorodiphenylsulfone with lithium sulfide was carried out. The progress of the polymerization can be monitored by NMR. However, the molecular weights of the hydrophilic poly (phenylene sulfide sulfone) precursor blocks (SS_v) cannot simply be evaluated by ^{1}H NMR since it is challenging to isolate oligomers with lithium aryl thiolate end-groups. In the case of end-functionalizing the precursor blocks

with frequently used coupling agents (e.g., C_6F_6, $C_{12}F_{10}$) the signals of the end-groups overlap with the signals of the block core. To overcome this disadvantage we have designed the novel coupling agent BPAF10 with which both ends of the precursor blocks are end-functionalized. Thus, the molecular weight of the precursor blocks can now be determined with ^{1}H NMR using the signals of the methyl protons of BPAF10 as an internal standard (signal of protons f compared to signal of protons a in Figure 1a,b). After the polymerization is completed a 5-fold excess of BPAF10 is added. The completion of the end functionalization of the hydrophilic precursor blocks with BPAF10 was confirmed by ^{19}F NMR (Figure 1c).

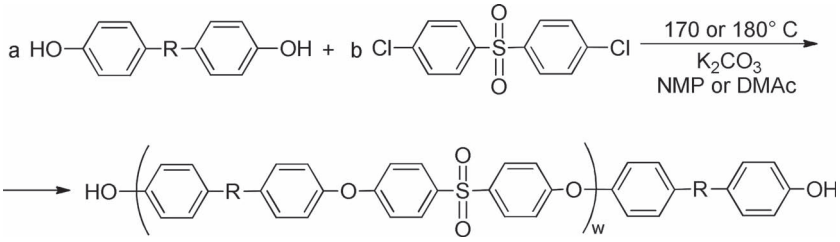

Scheme 3. Synthesis scheme of the hydrophobic blocks ES_w and FS_w. ES_w: R = -; FS_w: R = $C(CF_3)_2$.

By slightly varying the monomer ratio hydrophilic blocks with different molecular weights were obtained. Up to about 20 kDa there are no limitations in the synthesis of the hydrophilic precursor blocks. However, depending on the quality of the lithium sulfide (traces of water and disulfides) the target molar mass of the hydrophilic blocks can only be reproduced on the basis of test polymerizations with tiny variations of the stoichiometry.

Table 2. Characteristic data of the hydrophilic blocks SU_v and hydrophobic blocks ES_w and FS_w.

Hydrophilic	v	M_n[a)] [g mol^{-1}]	M_n[d)] [g mol^{-1}]	M_w[d)] [g mol^{-1}]	D [M_w/M_n][d)]
SU_9	9	5.4 k[b,c)]	16.6 k	24.1 k	1.5
SU_8	8	5.0 k[b,c)]	15.6 k	26.1 k	1.7
SU_{14}	14	7.4 k[b,c)]	21.8 k	31.5 k	1.5
Hydrophobic	**w**				
ES_{11}	11	4.4 k	6.4 k	11.4 k	1.8
FS_{13}	13	7.2 k	8.7 k	11.2 k	1.3
FS_{15}	15	8.3 k	9.4 k	13.9 k	1.5

[a)]Determined by ^{1}H NMR; [b)]Na^+-form of hydrophilic block; [c)]M_n differs from v times the molecular weight of the repeat unit (Table 1) because the hydrophilic blocks are end-functionalized with BPAF10; [d)]obtained from GPC in DMF at 60 °C.

The discrepancy between molar mass obtained by GPC and the NMR data can be attributed to the lack of appropriate calibration for the GPC analysis of the sulfonated precursor blocks. Therefore, we rely on the NMR-based data for the calculation of stoichiometry. As can be derived from Table 2, three different hydrophilic blocks with molecular weights (M_n) ranging from 5400 to 7400 with a rather narrow molecular weight distribution (polydispersity, PDI) were used for building the multiblock copolymers. The fact that the polydispersity of the sulfonated precursor blocks remains low even after end-capping with BPAF10 proves that there is no inter-molecular coupling during this reaction. The number of repeat units v (degree of polymerization) varies only between 9 and 14.

As fuel cell membranes are exposed to harsh conditions (T > 100 °C, extreme RH variations, possible formation of HO$^\bullet$ or $HO_2^\bullet$ radicals at the electrodes),[40] oxidative and hydrolytic stability plays an important role in their application. Polymers with sulfide (–S–) or ether (–O–) groups in the main chain are less stable than polymers with electron-withdrawing sulfone groups ($–SO_2$)[12,27] and their application in fuel cells is problematic.[41] To increase the oxidative and hydrolytic stability of the hydrophilic blocks we have oxidized the sulfonated poly

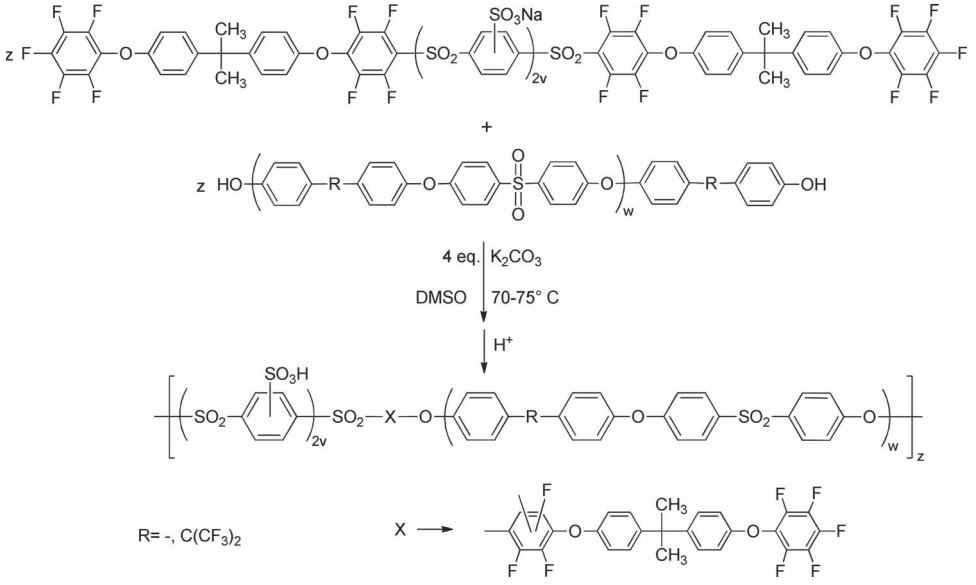

Scheme 4. Synthesis scheme of the multiblock copolymers SU_v-ES_w and SU_v-FS_w.

Table 3. Characteristic data of the multiblock copolymers SU_v-ES_w and SU_v-FS_w.

Multiblock Copolymer	z[a)]	M_n[b)] [g mol^{-1}]	M_w[b)] [g mol^{-1}]	D [M_w/M_n]	IEC[c)] [meq g^{-1}]	IEC[d)] [meq g^{-1}]	IEC[e)] [meq g^{-1}]
SU_9-ES_{11}	8	70.0 k	307.9 k	4.4	1.86	1.59	1.58
SU_8-FS_{13}	5	58.0 k	181.1 k	3.2	1.43	1.28	1.31
SU_{14}-FS_{15}	4	64.1 k	251.4 k	3.9	1.72	1.60	1.61

[a)] Number of hydrophilic-hydrophobic block sequences; [b)] obtained from GPC in DMF at 60 °C; [c)] theoretical; [d)] obtained from ^{1}H NMR; [e)] determined by titration with 0.1 N NaOH.

(phenylene sulfide sulfone) precursors (SS_v) to sulfonated poly (phenylene sulfone)s (SU_v) (Scheme 2). The structures and compositions of the SU_v-blocks were confirmed by ^{1}H, ^{13}C and ^{19}F NMR spectroscopy. The ^{1}H and ^{19}F NMR spectra of SS_v end-functionalized with BPAF10 and its corresponding oxidized form SU_v are shown in Figure 1. All NMR signals in coincide with the proposed chemical structure of the hydrophilic blocks, and an integration of the ^{1}H NMR signals rules out any significant change of molecular weight via side reactions in the course of the oxidation step.

3.2. Hydrophobic Blocks

As hydrophobic blocks two different types of poly(arylene ether sulfone)s have been synthesized via a step growth polymerization of the appropriate bis (hydroxyl phenylene) and bis(chlorophenyl) sulfone monomers. One contains a biphenyl unit (ES_w) and the other contains a hexafluoropropane biphenyl unit (FS_w) (Scheme 3).

Casting the multiblock copolymers to membranes we expected a better phase separation when using hexafluoropropane containing arylethersulfones (FS_w) caused by the stronger hydrophobicity of (FS_w) as compared to (ES_w).

Molecular weights were adjusted by choosing the appropriate starting monomer ratios. The number-average molecular weights were obtained from comparison of the ^{1}H NMR signal intensity of the end-groups with that of the backbone signals. The characteristic data of the hydrophobic blocks are summarized in Table 2. Three different hydrophobic blocks with molecular weights (M_n[a]) ranging from 4400 to 8300 and a rather narrow molecular weight distribution were used for building the multiblock copolymers.

3.3. Multiblock Copolymers

The multiblock copolymers, consisting of fully sulfonated poly (phenylene sulfone) blocks (SU_v) and hydrophobic poly(arylene ether sulfone) blocks (ES_w or FS_w), were synthesized via a multiple sequential coupling of the preformed hydrophilic with the hydrophobic blocks (Scheme 4). The coupling reaction is based on a nucleophilic aromatic substitution reaction between the phenoxide end-groups of the hydrophobic blocks and the BPAF10 end-groups of the hydrophilic blocks (sodium form). The average IECs of the multiblock copolymers were adjusted by choosing the appropriate hydrophilic to hydrophobic block length ratio v/w, while the molar ratios between the hydrophilic and hydrophobic blocks were carefully set as 1:1 to reach high total molecular weights.

It was found that the coupling reactions are very temperature sensitive. In the temperature range between 80 and 12 0 °C side reactions may occur which lead to gelation. The cross-linking most probably occurs between the phenoxide end-groups and fluorine functions in the backbone.[42] To meet these problems the reaction temperature for the coupling reaction via BPAF10 was set to 70–75 °C. This represents the lowest reaction temperature for such coupling reactions and gives rise to a minimum of crosslinking and high molecular weight multiblock copolymers (Table 3). All multiblock copolymers are soluble in common polar aprotic solvents such as NMP, DMF, DMSO and DMAc. The experimental values of the IECs were obtained by ^{1}H NMR and acid-base titration. The differences of experimental and theoretical IEC values might be caused by small deviations from the perfect 1:1 stoichiometry ratio of hydrophobic and hydrophilic blocks.

The multiblock copolymers consist of an alternating sequence of SU_v and ES_w or FS_w blocks, with the number of sequences varying between $4 \le z \le 8$ (a complete representation would be $[SU_v\text{-}ES_w]_z$ and $[SU_v\text{-}FS_w]_z$. However, for simplicity the multiblock copolymers are named only SU_v-ES_w and SU_v-FS_w in the following). This translates into a total molecular weight of the multiblock copolymers between $58\,000 \le M_n \le 70\,000$. This appears not very high compared to typical commercial poly(aryl ether sulfone)s, but it is sufficient when considering the rather challenging approach of coupling preformed blocks.

The values for z were calculated from the number average molecular weights obtained from GPC measurements and they present a rough estimation of the real molecular weights (molecular weights for hydrophilic and hydrophobic oligomers obtained from ^{1}H NMR data are lower than those obtained from GPC).

The structures and compositions of the multiblock copolymers were confirmed by ^{1}H, ^{13}C and ^{19}F NMR spectroscopy. The ^{1}H NMR spectrum of SU_{14}-FS_{15} is shown in **Figure 2**a as an example. The integration of the ^{1}H NMR signals clearly allows us to determine the content of hydrophilic and hydrophobic blocks in the multiblock copolymer.

In Figure 2b the ^{19}F NMR spectra of a multiblock copolymer and its corresponding starting hydrophilic block end-functionalized with BPAF10 are displayed. The fluorine signals from the pentafluorophenyl groups (3, 4, 5) are unchanged in the multiblock copolymer, while the intensity of the fluorine signals from the tetrafluorophenylene group (1, 2) are split. This indicates that the coupling takes place at the fluorinated benzene ring next to the hydrophilic block. From the chemical shift

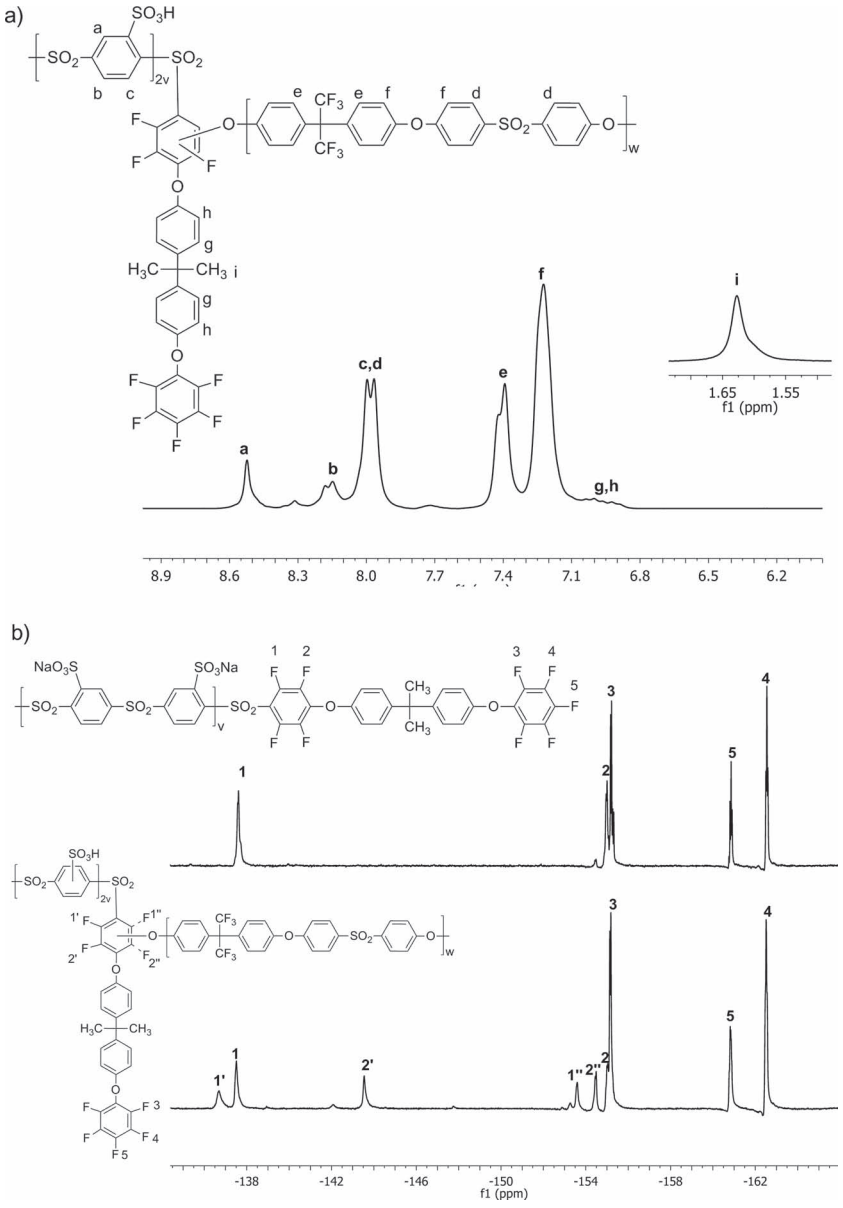

Figure 2. a) ^{1}H NMR spectrum of SU_{14}-FS_{15}. b) ^{19}F NMR spectra of SU_{14} blocks end-functionalized with BPAF10 (top) and SU_{14}-FS_{15} (bottom).

of the signals and their integrated intensity it can be concluded that the coupling of the hydrophobic blocks appears at the ortho- as well as at the meta-position to the sulfone group, with the ortho-position being preferred over the meta-position.

This can be explained in terms of the nucleophilic substitution reaction mechanism, because the electron-withdrawing group (-SO_2-) activates the ortho-position, while an electron donor group deactivates it.[43,44]

As a result of the NMR analysis the multiblock copolymers exhibit a rather unusual structure (Figures 2a,b). This is not only a result of the new coupling moiety BPFA10 being an integral part of the polymer structure, but is also due to its special binding geometry (as described in Figure 2). This may add some complexity to the phase separation since in addition with its strong hydrophobicity BPAF10 may act as "nucleus" for the phase separation process.

3.4. Thermal Properties

The thermal stability of the multiblock copolymers was evaluated by thermogravimetric analyses (TG) in dry nitrogen. A three-step weight loss is observed for all samples. The first loss of about 5–8 wt% up to 180 °C can be assigned to the loss of hydrated water, the second loss of about 10 wt% between 240 and 270 °C can presumably be attributed to desulfonation, and the third loss (>25 wt%) between 370 and 390 °C probably results from degradation of the polymer backbone. Differential scanning calorimetry (DSC) did not show any glass transition temperature below the onset of decomposition.

3.5. Membrane Morphology

Since our approach critically depends on the formation of a phase separated morphology, this was investigated by atomic force microscopy (AFM), transmission electron microscopy (TEM) and small angle x-ray scattering (SAXS). While AFM and TEM provide direct images of the distribution of soft (wet, hydrophilic) and hard (dry, hydrophobic) parts of the micro-structure in real space, SAXS accesses the corresponding correlation lengths in a quantitative way. The bright and dark regions seen in the tapping-mode atomic force micrographs (**Figure 3**a) correspond to the hard hydrophobic and soft hydrophilic domains. Although AFM is just probing the membrane surface, which may show some reconstruction effects, a clearly phase-separated morphology is visible with an extension of the soft (hydrophilic) domains falling into the range 8–15 nm. More distinct images are actually obtained by TEM on cross-sections of the membranes cut perpendicular to the surface.

The TEM image of a multiblock copolymer with larger block lengths shows a lamellar morphology with alternating parallel stripes formed by the hydrophilic and hydrophobic domains. The patterns very distinctly show the repetition length on the fracture surface ranging between approx. 11–16 nm (Figure 3b).

SAXS spectra of all multiblock copolymers show that the phase separations seen by AFM and TEM have distinct correlation lengths around d ≈ 15 nm (**Figure 4**). The narrow range is very surprising considering the different blocks lengths (see also Table 3). The typical length scales observed by microscopy and SAXS are actually smaller than the contour lengths of both

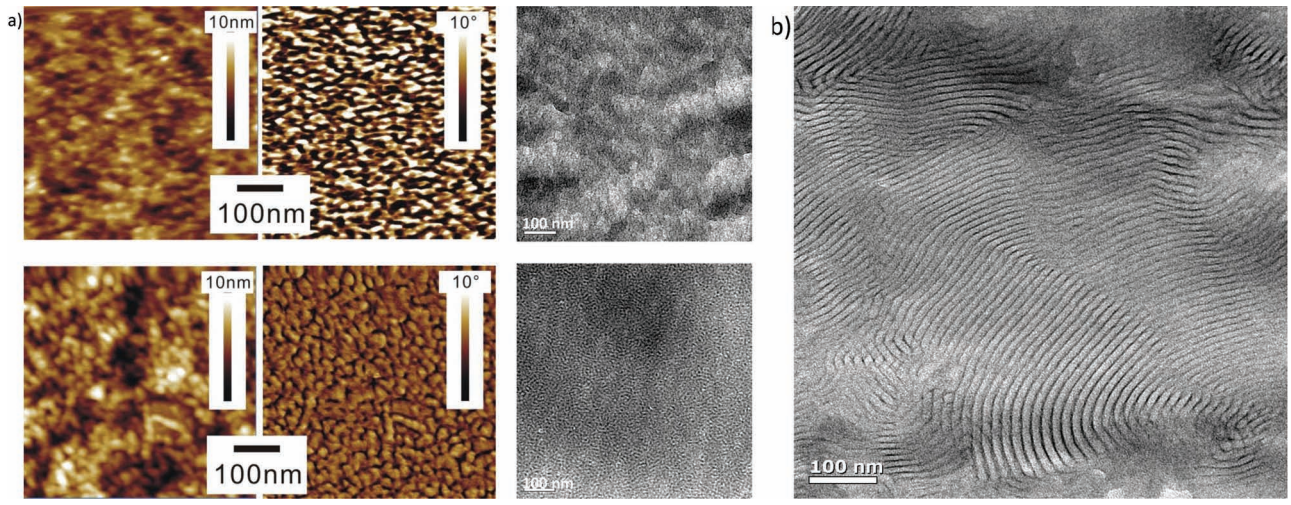

Figure 3. a) Microscopy images of multiblock copolymer membranes: AFM, surface topography contrast (left), AFM, surface phase contrast (center) and TEM of membrane cross-sections (right), upper row: SU_9-ES_{11}, lower row: SU_8-FS_{13}. b) TEM image of the cross-section of the multiblock copolymer SU_{14}-FS_{20}.

blocks, which are estimated to fall into the range of 14–23 nm for the hydrophilic and 23–34 nm for the hydrophobic blocks. Detailed information on the local conformations and the organization scheme of these multiblock copolymers are not available yet but are probably complex considering the unusual molecular structure (Figure 2a,b). It should be noted that the TEM pictures are obtained on dry films, while the SAXS spectra are recorded on humidified samples.

As shown recently, the kind of solvent and the degree of solvation may severely change the microstructure of these copolymers made of hydrophilic and hydrophobic sequences.[45]

Because of the limited q-range (<3 nm^{-1}) we can not yet decide whether the typical structure of the sulfonated poly (phenylene sulfone) (S-220) is maintained within the hydrated hydrophilic domain. However, as we will mention later, the advantageous properties of S-220 are virtually preserved within the hydrophilic volume increment of the microstructure.

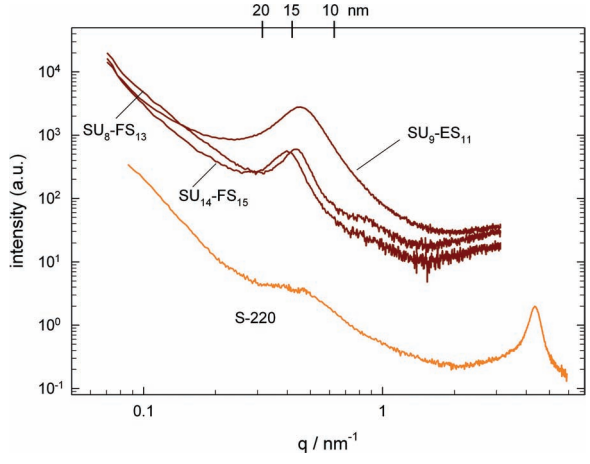

Figure 4. SAXS spectra of typical multiblock copolymers in the hydrated state (RH = 75%, $\lambda \approx 7$). The spectrum of pure S-220[35] is shown for comparison.

3.6. Water Uptake and Swelling

The water uptake of Polymer Electrolyte Membranes (PEM) is not only relevant for their proton conductivity but also for their mechanical stability.[46] High degrees of hydration typically lead to high conductivities, but also cause critical dimensional changes and very often reduce the morphological stability of the membranes dramatically. Therefore, balanced hydration behavior is necessary for the application as PEMs. This is the reason for focussing on multiblock copolymers with an IEC between of 1,2 to 1,7 meq/g in our present work.

Hydration only takes place within the hydrophilic domain, but the corresponding volume changes also affect the hydrophobic domain. The water uptake of the multiblock copolymers in terms of hydration number $\lambda = [H_2O]/[-SO_3H]$ as a function of temperature, and relative humidity (RH) is actually systematically lower than the corresponding data for Nafion (**Figure 5**a) up to RH = 65% ($\lambda \approx 5$) indicating a less negative free energy of hydration for the whole humidity range.

This is consistent with a much higher degree of water dispersion within the hydrophilic domain of the multiblock copolymer (similar to the situation in S-220) which may lead to a more negative entropy of hydration and therefore to a thermodynamic destabilization of the water of hydration. Since the data are recorded at constant RH as a function of temperature, the thermodynamic reference state is liquid water at the corresponding temperature. The slopes of λ versus T (RH = const.) should then be related to the heat of hydration with respect to this reference state. The fact that the slopes of λ versus T (RH = const.) for the multiblock copolymer and Nafion are very close also suggests similar heats of hydration for both materials. The hydration data for the three multiblock copolymers investigated in this work are actually very similar (data

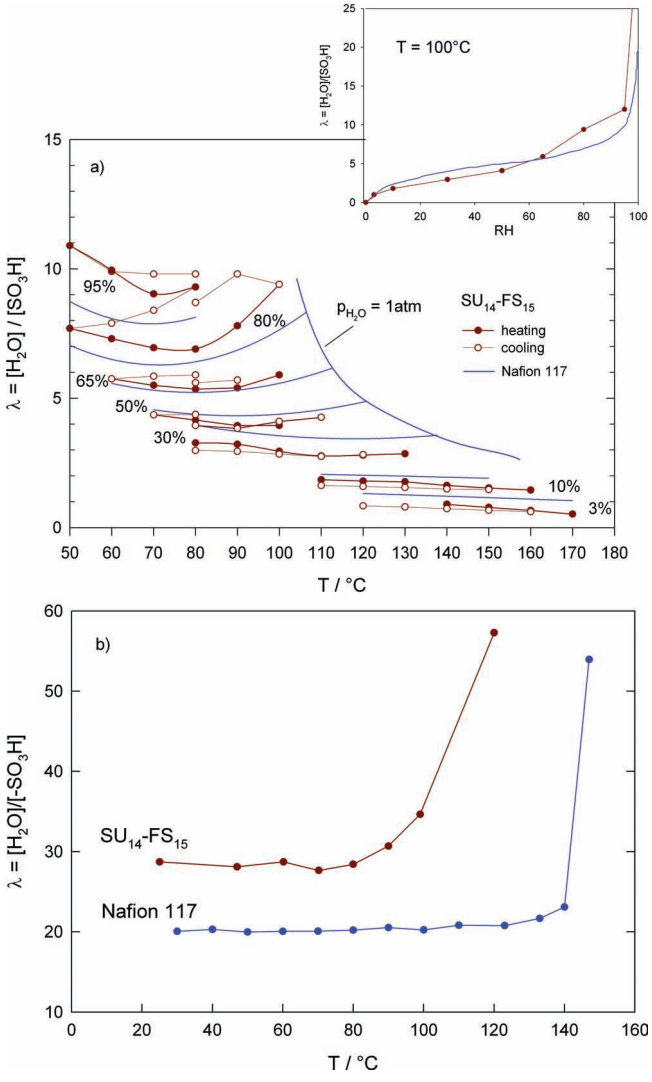

Figure 5. a) Water uptake $\lambda = [H_2O]/[-SO_3H]$ for different relative humidities RH as a function of temperature T. The data at T = 100 °C are represented as an isotherm in the insert. The data for Nafion including the water uptake in a pure water atmosphere ($p_{H2O} = 1$ atm) is given for comparison. b) Swelling of a multiblock copolymer and Nafion in pure water.

not shown). This is especially true for SU_9-ES_{11} and SU_{14}-FS_{15}; for SU_8-FS_{15}, hydration in terms of λ is also very similar, but because of the lower IEC, the absolute water uptake is correspondingly lower. A detailed thermodynamic analysis is currently in progress.

Although the water uptake per sulfonic acid group is smaller in the case of multiblock copolymers compared to Nafion for low RH, the absolute local water uptake within the high IEC hydrophilic domain is still significantly higher than that in Nafion.

As will be discussed below, the swelling which goes along with hydration lowers the elastic modulus. This in turn further increases swelling to the point at which the swelling pressure equals the elastic counter pressure mainly emerging from the deformation of the unsulfonated, hydrophobic domain. This effect becomes significant close to the dew point of water, where the swelling pressure severely increases as a consequence of osmosis, while the elasticity of the hydrophobic domain decreases.

In the case of S-220, this eventually leads to the dissolution of the polyelectrolyte, but the present multiblock copolymers keep their morphological integrity even when immersed in water (Figure 5b). This convincingly demonstrates that the hydrophobic poly(phenylene ether sulfone) segments form a continuous phase with sufficient morphological stability to sustain the internal swelling pressure.

3.7. Viscoeleastic Properties

The storage modulus as obtained by DMA is higher than 300 MPa at 90% RH which is more than twice the value for Nafion (**Figure 6**). As in the case of Nafion, the storage modulus very much depends on the level of humidification. This indicates that the properties of both, hydrophobic and hydrophilic domains are involved in the overall viscoeleastic behavior, which is supported by the observation that the overall dimensional changes (the linear dimensions of the sample were also recorded during the DMA runs) are consistent with the variations of the water volume fraction. Therefore, we can rule out that the hydrophilic domains swell and de-swell within the pores of a rigid hydrophobic matrix. As we will mention later, this is of particular importance for obtaining high proton conductivity at low levels of hydration. At high RH, the overall viscoelastic properties are probably dominated by those of the hydrophobic domains, which are weakened by the very strong local swelling of the sulfonated domains. With decreasing RH however, the increasing strength and brittleness of the hydrophilic domains also show up in the overall properties. At RH = 50%, the storage modulus of SU_{14}-FS_{15} approaches a value of 1 GPa at room temperature, which is factor of 5 higher than the value for Nafion (Figure 6). Under these RH conditions, the storage modulus actually decreases greatly with temperature. This is consistent with a redistribution of the hydration water within the hydrophilic domains that goes along with a loss of strength, as will be shown in a forthcoming publication. It should be noted at this stage that for the block lengths and IECs chosen for the present materials, brittleness at low RH may still be a problem for fuel cell applications, but these properties can be tuned continuously to meet the requirement of a particular application. More importantly, the storage modulus of this type of multiblock copolymers remains high, far beyond T = 100 °C where the mechanical properties of Nafion dramatically decay (Figure 6, left inset). Under relatively dry conditions (air), the softening of the hydrophobic domain is indicated by the sharp decay of the storage modulus at T ≈ 200 °C (Figure 6, right inset).

3.8. Transport Properties (Conductivity, Diffusion, Electro-Osmotic Drag)

Apart from the morphological stability, proton conductivity and water transport are key properties for the use of such membranes in electrochemical cells. For the multiblock copolymers

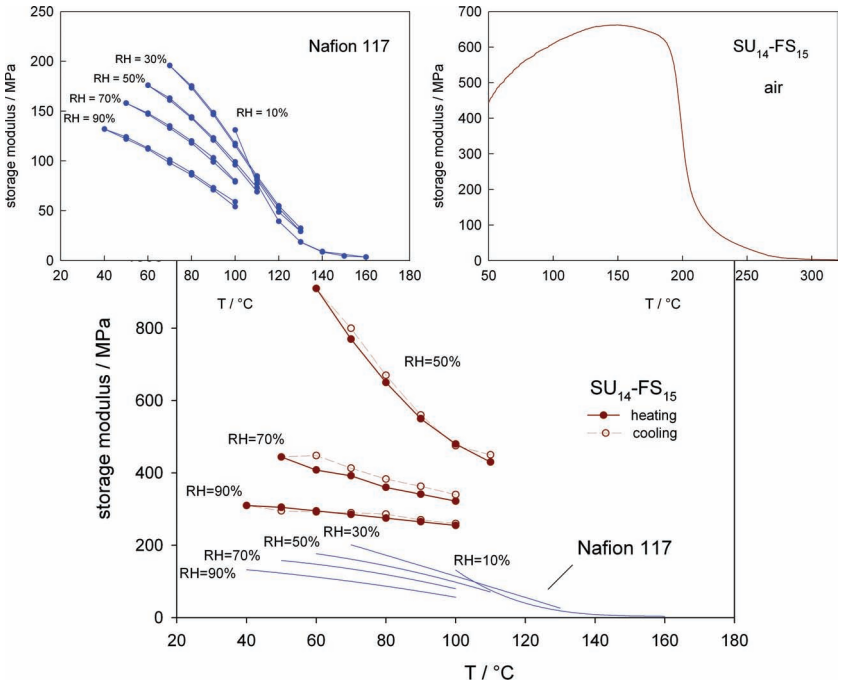

Figure 6. Storage modulus of the multiblock copolymer SU_{14}-FS_{15} as a function of RH and T. The data for Nafion are given for comparison. The two insets separately show the data for Nafion (left) and the storage modulus for SU_{14}-FS_{15} recorded in air (right).

with the highest IEC (SU_{14}-FS_{15} which has an IEC of 1.61 meq g^{-1}), the proton conductivity at high *T* and a constant water partial pressure of p_{H2O} = 1 atm is distinctly lower than the conductivity of pure S-220, but still slightly higher than the conductivity of Nafion (**Figure 7**a).

Compared to the conductivity of a statistically sulfonated poly (phenylene sulfone) copolymer (sPSO2–781), the conductivity is about an order of magnitude higher, clearly demonstrating the advantageous effect of concentrating the sulfonic acid functions into a continuous proton conducting domain.

The overall conductivity decrease compared to S-220 is expected from the decrease of charge carrier concentration (≈ factor of 3) and the decrease in percolation due to the presence of ≈60 vol% inert phase (≈ factor of 2). Locally, the advantageous conductivity properties of pure S-220 seem to be fully preserved within the hydrophilic SU_v domains as indicated by similar activation enthalpies for the conductivities of multiblock copolymers and pure S-220. As a result of the very high dispersion of water in S-220 (narrow water structures), the activation enthalpy for proton conductivity is higher than in PFSA membranes (such as Nafion).[35] As an example, the reader may refer to the conductivities of S-220 (λ = 4.9) and SU_{14}-FS_{15} (λ = 4.7) (Figure 7b). The activation enthalpies (temperature dependence) are similar, but the absolute conductivity of the multiblock copolymer is significantly lower and even below that of Nafion at low temperature.

However at high temperature, the conductivity of SU_{14}-FS_{15} is slightly higher than that of Nafion (Figure 7a,b) as a result of the higher activation enthalpy.

At room temperature, we recorded the conductivity for many more hydration numbers λ, and the conductivity diffusion coefficients D_σ obtained from these data via the Nernst-Einstein relationship are compared to the water tracer diffusion coefficient D_{H2O} (**Figure 8**). This provides direct information on how the mobility of protonic charge carriers is related to the diffusion of water. As in the case of PFSA membranes (e.g., Nafion), both transport coefficients are virtually identical at low levels of hydration, suggesting that the charge carriers are essentially hydrated excess protons (e.g. H_3O^+, $H_5O_2^+$), which are mobile as a whole without significant intermolecular proton transfer. With increasing hydration D increases more than D_{H2O} which is generally explained by the appearance of structure diffusion involving intermolecular proton transfer.[2] The principle behavior is reminiscent of PFSA membranes and plain aqueous solutions of acids.[47] However, both transport coefficients decrease more severely with decreasing hydration (Figure 8), probably as a consequence of increasing activation enthalpies as the differences tend to level off at high temperatures (Figure 7).

This is surprising considering that the local water volume fraction within the hydrophilic domain is more than twice that of Nafion (for the same overall water volume fraction). But the much higher degree of water dispersion within this domain seems to increase the activation enthalpy of water diffusion and proton mobility as in the case of pure S-220.[35]

Another consequence of the high degree of water dispersion within the proton conducting SU_v domains of the multiblock structure is the absence of any significant hydrodynamic water transport. This is related to a very low electro-osmotic drag coefficient, which we were able to measure for the first time for poly(phenylene sulfone) based materials. As anticipated from the particular microstructure of high IEC materials,[35] the electroosmotic water drag (K_{drag}) is distinctly lower than that of Nafion. This applies even for a given hydration number λ (**Figure 9**a), which can be taken as an approximate parameter for the relative humidity RH (see Figure 5). Because of the very high IEC of the poly(phenylene sulfone)s however, a given hydration number λ corresponds to a much higher water volume fraction, and the large differences of K_{drag} in the plot versus water volume fraction (Figure 9b) reflect the fundamentally different distribution of water in both types of ionomers (polyelectrolytes). The fact that the data for the multiblock copolymers correspond to the trend of the S-220 data is additional support for the conclusion that the properties of S-220 are approximately preserved in the local properties of the SU_v hydrophilic domains of the multiblock structure.

4. Summary and Outlook

We successfully prepared a series of muliblock copolymeres containing highly sulfonated poly phenylene sulfones (SU_v,

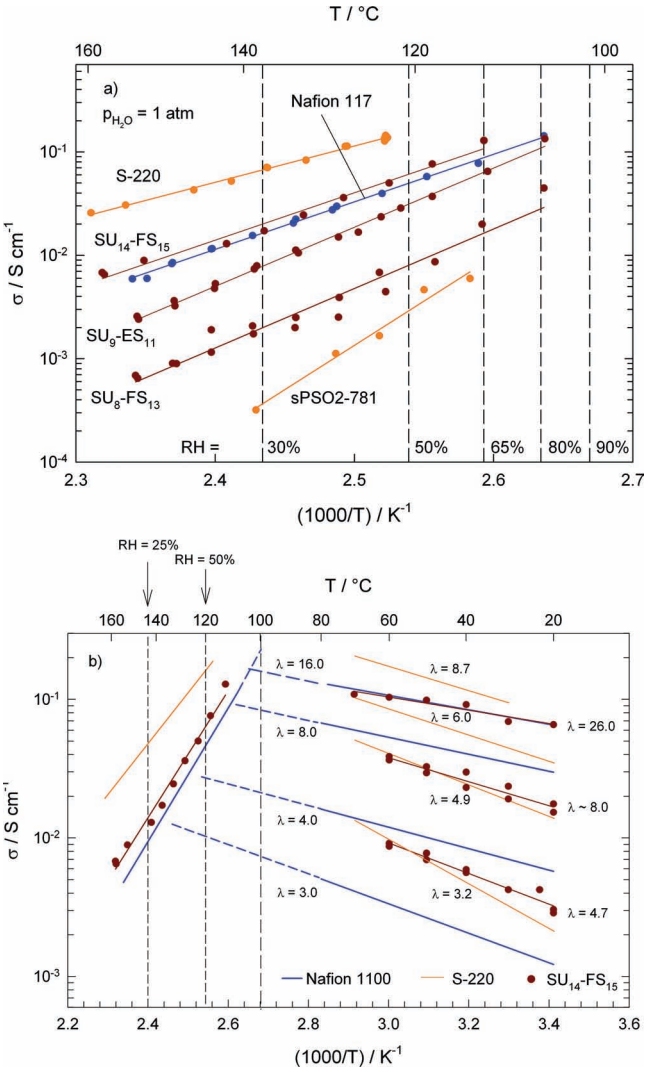

Figure 7. Proton conductivity of the multiblock copolymers in a water atmosphere (the conductivities of pure S-220[35] and Nafion are given for comparison): a) At constant water pressure (p_{H2O} = 1 atm). Note that the conductivity of a statistical sulfonated poly phenylene sulfone copolymer (sPSO2–781) of similar IEC (1.4 meq g^{-1})[27] is significantly lower. b) SU_{14}-FS_{15} at low temperature at constant λ, at high temperature at a constant water pressure (p_{H2O} = 1 atm).

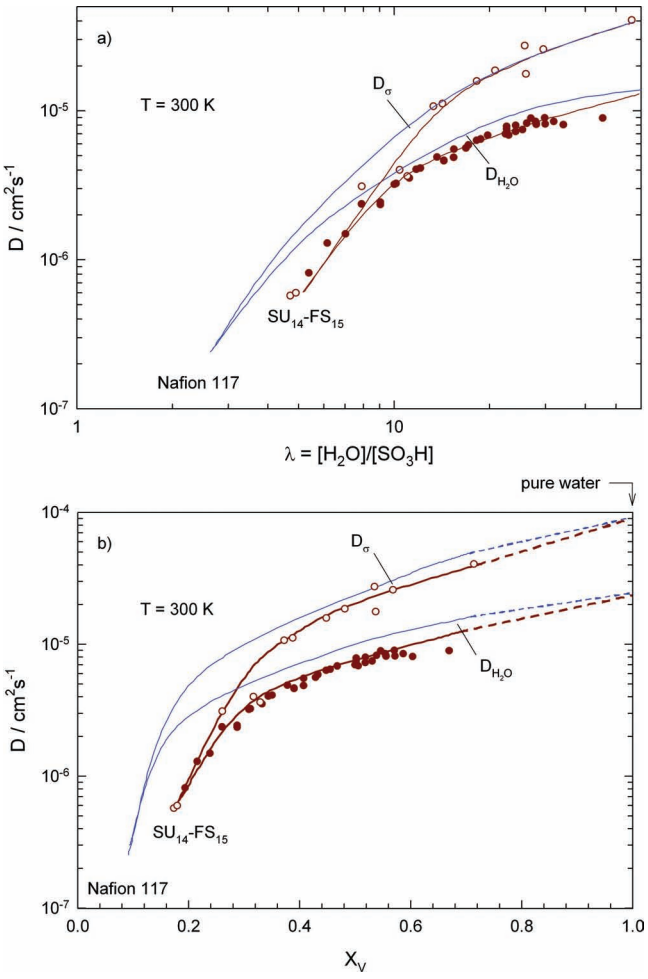

Figure 8. Comparison of the conductivity diffusion coefficient $D_σ$ and water tracer diffusion coefficient D_{H2O} at room temperature as a function of the hydration number λ (a) and as a function of water volume fraction X_V (b). The data for Nafion[2] are shown for comparison.

IEC = 4.5 meq g^{-1}) as hydrophilic segments. The total IEC ranges from 1.2 to 1.7 meq g^{-1} corresponding to approx. 40–60 vol% of the unsulfonated inert phase. If cast from solution, distinct phase separation with correlation lengths around 15 nm are observed. As a consequence, the membranes combine high proton conductivity with advantageous viscoelastic properties. Especially at high temperatures, proton conductivity is slightly higher than that of Nafion and no softening is observed. The results clearly demonstrate that highly sulfonated poly (phenylene sulfone), which, as a pure phase, is brittle in the dry state and water soluble at high RH, is successfully used as constituent of phase separated membranes with reasonable viscoelastic properties. Locally, the advantageous transport properties (high proton conductivity, low electro-osmotic water drag) are preserved in continuous hydrophilic phases which still allow for efficient proton conductivities significantly higher than those of sulfonated poly(phenylene sulfone) statistical copolymers.

Since the hydrophilic segments exclusively contain acceptor substituted phenyl rings, we assume that the superior hydrolytic stability of S-220 homopolymer[34] is maintained within the multiblock copolymer as well.

Thanks to their well separated microstructure, the superior transport and stability properties of their proton conducting hydrophilic phase and the morphological stability of their hydrophobic phase, these multiblock copolymers have a great potential to substitute for PFSA membranes used as separator materials in electrochemical applications such as PEM fuel cells and redox flow batteries.

However, the distinctly different chemical nature and the significantly lower hydrodynamic water transport also require that the other components in such applications be adjusted to this new type of membrane. For fuel cell applications this also

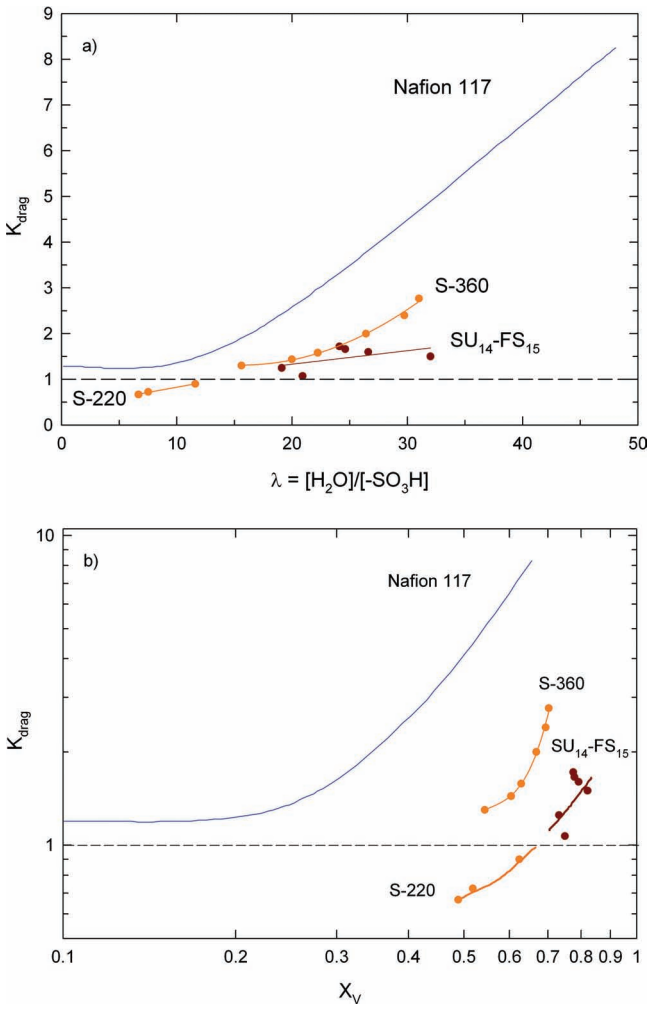

Figure 9. Electroosmotic drag coefficients (K_{drag}) for Nafion,[2] S-360 (half sulfonated poly phenylene sulfone[27]), S-220 and SU_{14}-FS_{15} as a function of λ (a) and water volume fraction X_v (b). Since the electro-osmotic drag is closely related to the local water content, the data for the multiblock copolymer are plotted versus the water volume fraction of the hydrophilic S-220 domain.

includes the electrode structures and the process of joining them with the membrane.

5. Experimental Data

5.1. Bisphenol-A-bis (pentafluorophenyl)ether (BPAF10)

^{1}H NMR (250 MHz, DMSO-d_6, δ): 1.62 (s, 6H_c), 7.02 (d, 4H_b, J = 8.8 Hz), 7.21 (d, 4H_a, J = 8.9 Hz). ^{13}C NMR (125.76 MHz, DMSO-d_6, δ): 31.3 (s), 42.5 (s), 115.3 (s), 128.6 (s), 130.2 (m), 137.6 (m), 138.1 (m), 139.6 (m), 140.1 (m), 141.6 (m), 143.5 (m), 146.5 (s), 155.5 (s). In ^{13}C NMR spectra signals of the pentafluorophenyl fragments are weak and appear as multiplets due to the strong coupling with fluorine. ^{19}F (470.59 MHz, DMSO-d_6, δ): –153.1 (d, 4F_3), –159.1 (t, 2F_1), –161.3 (t, 4F_2). MALDI-TOF: m/z (%) 561.2 (100).

5.2. Sulfonated Poly(phenylene sulfide sulfone) Precursor block (SS_v) End-Functionalized with BPAF10

^{1}H NMR (250 MHz, DMSO-d_6, δ): 1.64 (H_f), 7.03 (H_e), 7.16 (H_d), 7.28 (H_c), 7.79 (H_b), 8.31 (H_a). ^{13}C NMR (75.47 MHz, DMSO-d_6, δ): 30.4, 41.6, 114.6, 114.9, 128.1, 128.8, 129.2, 131.2, 141.5, 142.9, 143.0, 143.4, 144.2, 145.7, 146.0, 146.5, 147.2, 147.6, 154.4, 154.6. ^{19}F (470.59 MHz, DMSO-d_6, δ): –131.5 (d, 2F_1), –152.2 (d, 2F_2), –154.5 (d, 2F_3), –160.1 (t, 1F_5), –161.8 (t, 2F_4), (Figure 1a, 1c). The signals at 7.6–7.7 ppm and around 8.2 ppm in Figure 1a, and at 8.3 ppm in Figure 1b can be attributed to the protons of the benzene ring directly linked to the BPAF10 since they appear at different chemical shifts than the signals of the main polymer backbone.

5.3. Sulfonated Poly(phenylene sulfone) Block (SU_v) End-Functionalized with BPAF10

^{1}H NMR (250 MHz, DMSO-d_6, δ): 1.63 (H_f), 7.04 (H_e), 7.22 (H_d), 7.98 (H_c), 8.17 (H_b), 8.52 (H_a). ^{13}C NMR (75.47 MHz, DMSO-d_6, δ): 30.4, 41.7, 114.6, 114.9, 128.1, 128.8, 129.2, 131.2, 142.9, 143.0, 143.1, 143.2, 144.2, 145.6, 146.0, 146.5, 147.6, 154.4, 154.6. ^{19}F (470.59 MHz, DMSO-d_6, δ): –136.8 (d, 2F_1), –154.2 (d, 2F_2), –154.4 (d, 2F_3), –160.1 (t, 1F_5), –161.7 (t, 2F_4) (Figure 1b, 1d).

5.4. Poly(arylene ether sulfone) Block (ESw)

^{1}H NMR (250 MHz, DMSO-d_6, δ): 6.85 (end-group, d), 7.17 (4H and end-group, m), 7.46 (end-group, d), 7.62 (end-group, d), 7.73 (2H, d), 7.95 (2H, d). ^{13}C NMR (63 MHz, DMSO-d_6, δ) 115.8, 118.0, 120.7, 127.5, 128.5, 129.9, 135.3, 136.0, 154.1, 161.2.

5.5. Poly(arylene ether sulfone) block (FS_w)

^{1}H NMR (250 MHz, DMSO-d_6, δ): 6.85 (end-group, d), 7.14 (end-group, d), 7.24 (4H, m), 7.41 (2H, d), 7.99 (2H, d). ^{13}C NMR (63 MHz, DMSO-d_6, δ) 119.0, 119.6, 128.1, 130.0, 131.8, 136.0, 155.7, 160.2.

Acknowledgements

The authors thank M. G. Marino and A. Wohlfarth (both MPI-FKF) for critically reading the proofs, G. Portale (European Synchrotron Radiation Facility, Dubble beam line) for his support during the SAXS experiments, and U. Klock and A. Fuchs (both MPI-FKF) for technically supporting the TGA and DMA measurements. The optimization of the synthesis by A. Manhart is very much acknowledged as well as the technical support by R. Berger and H. Burg for the AFM and by I. Lieberwirth for the TEM investigations (all MPI-P). The authors are also very thankful for the generous financial support of the project "PSUMEA" by the Bundesministerium für Wirtschaft (BMWi) under the contract number 03ET2004A/B, Energie Baden-Württemberg (EnBW) and Fumatech.

Received: March 22, 2012
Revised: May 22, 2012
Published online: June 25, 2012

[1] L. Ghassemzadeh, K. D. Kreuer, J. Maier, K. Müller, *J. Phys. Chem. C* **2010**, *114*, 14635.
[2] K. D. Kreuer, S. J. Paddison, E. Spohr, M. Schuster *Chem. Rev.* **2004**, *104*, 4637.
[3] B. C. H. Steele, A. Heinzel, *Nature* **2001**, *414*, 345.
[4] M. A. Hickner, H. Ghassemi, Y. S. Kim, B. R. Einsla, J. E. McGrath, *Chem. Rev.* **2004**, *104*, 4587.
[5] M. F. Mathias, R. Makharia, H. A. Gasteiger, J. J. Conley, T. J. Fuller, C. J. Gittleman, S. S. Kocha, D. P. Miller, C. K. Mittelsteadt, T. Xie, S. G. Yan, P. T. Yu, *Electrochem. Soc. Interface* **2005**, *14*, 24.
[6] K. D. Kreuer, Hydrocarbon membranes. In *Handbook of Fuel Cells - Fundamentals, Technology and Applications. Volume 3: Fuel Cell Technology and Applications; Part 1*, (Eds: W. Vielstich, A. Lamm, H. Gasteiger), John Wiley & Sons Ltd., Chichester, UK **2003**.
[7] J. Roziere, D. J. Jones, *Annu. Rev. Mater. Res.* **2003**, *33*, 503.
[8] Q. Li, R. He, J. O. Jensen, N. J. Bjerrum, *Chem. Mater.* **2003**, *15*, 4896.
[9] M. Rikukawa, K. Sanui, *Prog. Polym. Sci.* **2000**, *25*, 1463.
[10] G. Maier, J. Meier-Haack, *Adv. Polym. Sci.* **2008**, *216*, 1.
[11] K. D. Kreuer, *J. Membr. Sci.* **2001**, *185*, 29.
[12] G. Titvinidze, A. Kaltbeitzel, A. Manhart, W. H. Meyer, *Fuel Cells* **2010**, *10*, 390.
[13] W. L. Harrison, M. A. Hickner, Y. S. Kim, J. E. McGrath, *Fuel cells* **2005**, *5*, 2001.
[14] H.-S. Lee, A. Roy, O. Lane, M. Lee, J. E. McGrath, *J. Polym. Sci., Part A: Polym. Chem.* **2010**, *48*, 214.
[15] H.-S. Lee, A. Roy, O. Lane, S. Dunn, J. E. McGrath, *Polymer* **2008**, *49*, 715.
[16] Y. Li, A. Roy, A. S. Badami, M. Hill, J. Yang, S. Dunn, J. E. McGrath, *J. Power Sources* **2007**, *172*, 30.
[17] H.-S. Lee, A. Roy, A. S. Badami, J. E. McGrath, *Macromol. Res.* **2007**, *15*, 160.
[18] H.-S. Lee, A. S. Badami, A. Roy, J. E. McGrath, *J. Polym. Sci., Part A: Polym. Chem.* **2007**, *45*, 4879.
[19] C. Vogel, H. Komber, A. Quetschke, W. Butwilowski, A. Pötschke, K. Schlenstedt, J. Meier-Haack, *Reactive Funct. Polym.* **2011**, *71*, 828.
[20] X. Yu, A. Roy, S. Dunn, J. Yang, J. E. McGrath, *Macromol. Symp.* **2006**, *245–246*, 439.
[21] T. Mikami, K. Miyatake, M. Watanabe, *J. Polym. Sci., Part A: Polym. Chem.* **2011**, *49*, 452.
[22] B. Bae, K. Miyatake, M. Uchida, H. Uchida, Y. Sakiyama, T. Okanishi, M. Watanabe, *ACS Appl. Mater. Interfaces* **2011**, *3*, 2786.
[23] B. Bae, K. Miyatake, M. Watanabe, *ACS Appl. Mater. Interfaces* **2009**, *1*, 1279.
[24] K. Nakabayashi, T. Higashihara, M. Ueda, *J. Polym. Sci., Part A: Polym. Chem.* **2010**, *48*, 2757.
[25] Y. A. Elabd, M. A. Hickner, *Macromolecules* **2011**, *44*, 1.
[26] Y. Fan, M. Zhang, R. B. Moore, H.-S. Lee, J. E. McGrath, *Polymer* **2011**, *52*, 3963.
[27] M. Schuster, K. D. Kreuer, H. T. Anderson, J. Maier, *Macromolecules* **2007**, *40*, 598.
[28] S. Takamuku, P. Jannasch, *Macromol. Rapid Commun.* **2011**, *32*, 474.
[29] S. Takamuku, P. Jannasch, *Adv. Energy Mater.* **2012**, *2*, 129.
[30] C. Iojoiu, M. Marechal, F. Chabert, J.-Y. Sanchez, *Fuel Cells* **2005**, *5*, 344.
[31] J. F. Blanco, Q. T. Nguyen, P. Schaetzel, *J. Appl. Polym. Sci.* **2002**, *84*, 2461.
[32] P. Jannasch, *Fuel Cells* **2005**, *5*, 248.
[33] G. Titvinidze, K. D. Kreuer, W. H. Meyer, *18th Int. Conf. Solid State Ionics*, Warsaw (Poland), July 3–8, **2011**.
[34] M. Schuster, C. C. de Araujo, V. Atanasov, H. T. Andersen, K. D. Kreuer, J. Maier, *Macromolecules* **2009**, *42*, 3129.
[35] C. C. de Araujo, K. D. Kreuer, M. Schuster, G. Portale, H. Mendil-Jakani, G. Gebel, J. Maier, *Phys. Chem. Chem. Phys.* **2009**, *11*, 3305.
[36] Z. G. Wang, T. L. Chen, J. P. Xu, *Polym. Int.* **2001**, *50*, 249.
[37] S. Takamuku, K. Akizuki, M. Abe, H. Kanesaka, *J. Polym. Sci., Part A: Polym. Chem.* **2009**, *47*, 700.
[38] F. Bauer, S. Denneler, S. Willert-Porada, *J. Polym. Sci. B* **2005** *43*, 786.
[39] M. Ise, K. D. Kreuer, J. Maier, *Solid State Ionics* **1999**, *125*, 213.
[40] D. Xing, J. Kerres, *Polym. Adv. Technol.* **2006**, *17*, 591.
[41] K. Goto, I. Rozhanskii, Y. Yamakawa, T. Otsuki, Y. Naito, *Polym. J.* **2009**, *41*, 95.
[42] X. Yu, A. Roy, S. Dunn, A. S. Badami, J. Yang, A. S. Good, J. E. McGrath, *J. Polym. Sci., Part A: Polym. Chem.* **2009**, *47*, 1038.
[43] J. Ding, F. F. Liu, M. Li, M. Day, M. Zhou, *J. Polym. Sci., Part A: Polym. Chem.* **2002**, *40*, 4205.
[44] K. Kimura, Y. Tabuchi, Y. Yamashita, P. E. Cassidy, J. W. Fitch III, Y. Okumura, *Polym. Adv. Technol.* **2000**, *11*, 757.
[45] S. Yakovlev, X. Wang, P. Ercius, N. P. Balsara, K. H. Downing, *J. Am. Chem. Soc.* **2011** *133*, 20700.
[46] T. A. Zawodzinski, T. E. Springer, J. Davey, R. Jestel, C. Lopez, J. Valerio, S. Gottesfeld, *J. Electrochem. Soc.* **1993**, *140*, 1981.
[47] Th. Dippel, K. D. Kreuer, *Solid State Ionics* **1991**, *46*, 3.